ISSN 1110-0354
Bull. Nat. Inst. Of Oceanogr. & Fish., A.R.E., 2000. Vol. (26): 43 - 70

TRACING SOME WATER QUALITY AFTER THE CONSTRUCTION OF EL-DEKHELA NEW HARBOUR USING REMOTE SENSING

BY

FARAG, M. M.; ABOUL-NAGA, W. M.; SHALABY, E. A.; BAGHDADI, H. H. AND KAMEL, M. S.*

**Institute of Graduate Studies and Research. University of Alexandria. Egypt.*

Key Words: El-Dekhela New Harbour, Total suspended matter, Transparency, Salinity.

ABSTRACT

Studies were made in El-Dekhela and El-Mex regions, but special studies are needed to understand the variability of the water quality (total suspended matter, TSM, transparency and salinity) after the construction of the New Harbour. Therefore, the objective of this study is to use the remote sensing application on marine environment for detecting transparency, salinity and total suspended matter and its influences on El-Mex Bay and El-Dekhela Harbour based on the integration of Landsat MSS imagery.

Remote sensing techniques assess the water quality in El-Mex Bay and El-Dekhela Harbour with special algorithms to extract all possible information using Landsat MSS imagery (bands 4, 5, 6 and 7). The resulted images have been compared with ground measurements and showed high agreement significant relation between them. The construction of El-Dekhela New Harbour makes the area more closed and the harbour prevents the renew of water, so the TSM and transparency have been increased while S‰ decreased.

INTRODUCTION

Alexandria city, which is considered the main summer resort in Egypt, lies on the southern coast of the Eastern Mediterranean Sea, to the west of the Nile Delta (Fig.1). It has a population of more than five millions (Central Authority for Mobilization and Statistics, CAMS, 1996). It has also a great economic importance to Egypt where about 90% of Egyptian export and import activities are done through Alexandria (Alexandria Port Authority, APA, 1996).

The study area covers the Western Harbour, El-Mex Bay and El-Dekhela Harbour lies at the west of Alexandria between latitudes 31° 07` N; 31 31` N and longitudes 29° 47` E; 29° 53` E. The Western Harbour proper is elliptical in shape having a length of 7 km and a maximum width of 2 km (Alexandria Port Authority, APA, 1996). El-Dekhela Harbour was planned in 1985 to serve Alexandria Iron and Steel Factory. It lies to the east of El-Agami head land and to the west of El-Mex Bay (Fig. 1), and its depth varying from 6 to 19 m with a mean of 12.4 m. The harbour structure consists of four quays. The northwestern side of the harbour is bordered by an artificial wave brake which is about 2.5 km long (Abd-Alla ***et al.***, 1995).

The pollutants on the study area can be divided into two classes: petroleum pollution and non-petroleum pollution (Halim, 1983 and Nessim, 1994). These pollutants have a severe effect on the water quality and the associated aquatic ecosystem. Traditional methods used for monitoring surface water quality may give possible information but it is expensive and can't provide continuous monitoring. Remote sensing techniques are a powerful tool for detecting pollution providing quantitative information about concentrations, locations and its influences on the marine environment (Robinson, 1985). These information are important for the decision-makers, which are responsible for environmental protection policies.

Derivation of water quality algorithms based on statistical correlation between the remote sensing measurements and field measurement (Cracknell ***et al.***, 1988). Total suspended matter, transparency and salinity have been detected and quantified by remote sensing with varying degrees of success and then different algorithms have applied various degrees of success. Water quality studies depending on the chemical analysis methods of random seawater

specimens by Aboul-Dahab ***et al.*** (1984) and Aboul-Dahab (1985), Emara ***et al.***(1984), Said ***et al.***(1991), Tayel ***et al.***(1996) and Fahmy ***et al.***(1997) indicated high changes in water quality (transparency, salinity and total suspended matter, TSM) after El-Dekhela Harbour planning.

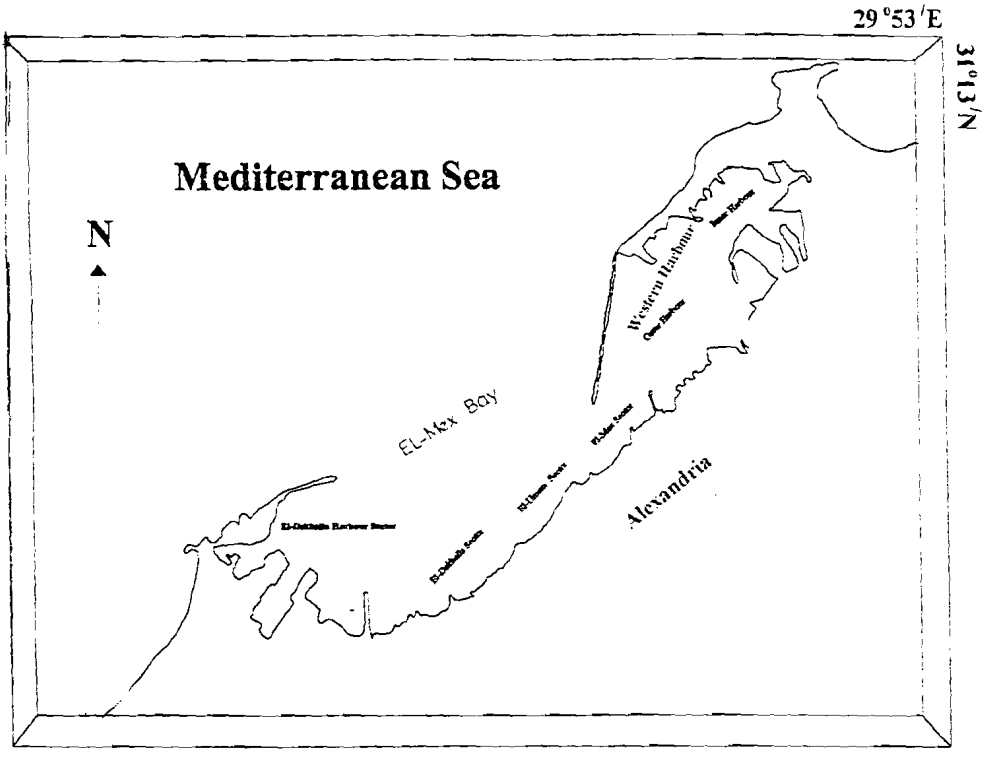

Fig. (1): Study Area

2. Data acquisition

Primary data available for this study were monitoring water quality using Landsat MSS and field measurements. Two types of data have been used for this study; field data and satellite imagery of Landsat-MSS.

Table (2): Acquisition data at 1983, 1985 and 1991.

Date	Platform	Dimensions
31 July 1983	Landsat-3	671*253 Pixels
26 June 1985	Landsat-3	420*194 Pixels
19 February 1991	Landsat-4	585*333 Pixels

3. Monitoring and analysis techniques

The fundamental concepts of water quality remote sensing depend on the relationship between water quality and their interactions with electromagnetic spectra (Austin, 1974). Some techniques can be used by remote sensing for locating, identifying and mapping coastal features and pollutants. Recently, Schnider and Mauser (1996) and Kindratyev ***et al.***(1998) have established several modeling methods in water quality remote sensing.

3.1. Preprocessing techniques

A reference image was rectified onto a latitude/longitude grid through the use of 14 control points. Also, all interpolated maps of horizontal distribution of parameters (after converting them to raster) are registered to the Landsat MSS data using RESAMPLE module. After that, all the images and *in-situ* measurement were registered to the reference image using the mentioned software. The accuracy of registered images was valid. The image processing work was achieved in "Remote Sensing Image Processing and GIS Unit". Two integrated equipment were used; one of map digitization and the other for image processing containing image registration and land masking.

3.1.a. Image registration

In this work, we chose the image dated (19 February 1991) as the reference image because it was the best image.

3.1.b. Land masking

All land pixels were masked to avoid interference between land and water pixel values. Giving the value (0) for all land pixels does this mask; and then those pixels are excluded from all the calculations performed to the images.

3.1.c. Enhancement

All the images were enhanced by the same function to be useful for monitoring and comparing the different distribution features between different

dates. Linear stretch technique was applied to increase the contrast of the images and thereby enhance visual interpretation. Applying linear stretch leads to high tonal of light with value and dark pixels with value.

3.2. Water quality algorithms

We are going to introduce the algorithms which are used at this study and fitted our area.

3.2.a. Total suspended matter algorithm

TSM is a major factor affecting water quality in main aquatic ecosystem. This research is undertaken to determine the application of digital spectral data collected by Landsat MSS for estimating TSM in aquatic ecosystems, the following algorithm was designed and examined by Ritchie *et al.*(1987) and re-examined by Richardo (1993).

According to this logarithm, three bands 4, 6 and 7 are used to calculate TSM, as follows:

$$TSM = -34.86 + 2.44 * Band\ 4 + 6.94 * Band\ 6 - 3.55 * Band\ 7 \quad (mg\ \ell^{-1})$$

3.2.b. Transparency algorithm

This algorithm also based on Shimoda *et al.*(1986) works using the four bands of MSS as follows:

$$Transparency = 107.591 + 0.24165 * Band\ 4 - 0.634966 * Band\ 5 - 1.41489 * Band\ 6 + 1.31712 * Band\ 7 \quad (cm)$$

3.2.c. Salinity algorithm

This algorithm used Landsat MSS digital data to map salinity distribution in the study area. The following algorithm was designed and examined by Khorram and Cheshire (1985).

This algorithm used the visible region bands of Landsat MSS to derive the salinity:

$$Salinity = 38.524 - 120.858\ x\ \frac{Band6}{Band4 + Band5} \quad (‰)$$

Correlation matrix was produced for all water quality parameters and all four MSS bands and their somewhat typical band combinations and ratios.

The best regression fit for each one of the selected water quality parameters was determined based on root mean square error values, the residual value and the simplicity of the model.

4. Raster distribution of water quality

In this section all the ground measurements data will be introduced after converting them to raster data. This will help for comparison between the results from satellite imagery and these raster data. All ground measurements are converted by using the above spatial enhancement technique.

4.1. Total suspended matter distribution

Surface distribution of TSM referred to the measurements of Aboul-Dahab (1985) (August 1983 and August 1984) are shown in Figures (2 and 3), respectively.

In Fig. (2), the high level of TSM is found in El-Mex 1 region (9.2 mg ℓ^{-1} - the red colour), and decreased gradually in the direction of El-Dekhela region. In El-Mex 2 region, the level was 8.8 mg ℓ^{-1} (orange colour). In El-Dekhela region, the level decreased to 5.3 mg ℓ^{-1} (yellow colour), while in El-Dekhela Harbour region was the lowest value (2.8 mg ℓ^{-1} - green colour). This measurement was taken before the construction of El-Dekhela New Harbour.

In Fig. (3), high concentration of TSM was found in El-Mex 1 region (14.9 mg ℓ^{-1} - red colour), while low concentration was found in El-Dekhela region it was 4.22 mg ℓ^{-1} (very pale green colour). Figure 4 shows the surface distribution of TSM in August 1994 after Fahmy ***et al***. (1997). The TSM in El-Dekhela Harbour region increased in their levels comparing with recorded measurements by Aboul-Dahab (1985). In El-Mex 1 region, the concentration was 5.9 mg ℓ^{-1}, in El-Mex2 region and El-Dekhela Harbour region (very pale green) it was between 5.5-5.9 mg ℓ^{-1}, while, in El-Dekhela region (green colour) it was 4.5 mg ℓ^{-1}.

So, we can say that the increasing of TSM concentration is the result of increasing activity of the New Harbour and accumulation of the disposed load by El-Umum Drain.

4.2. Transparency distribution

Seawater transparency was determined twice: in August 1983 and August 1984, as shown in Figures (5 and 6), respectively, after Aboul-Dahab (1985).

Figure (5) showed that the transparency recorded in August 1983 had the lowest value in El-Mex 1 region 110 cm – green colour. In El-Mex 2 region, it was 160 cm (yellow colour), while in El-Dekhela region it was 240 cm (orange colour) and it increased in direction of El-Dekhela Harbour region up to 310 cm (pale red colour).

Figure (6), after Aboul-Dahab (1985), also, showed that the transparency in El-Mex 1 region was 80 cm (green colour), El-Mex 2 region 180 cm (pale green colour) and in a small part in El-Dekhela Harbour region it was found that the transparency was 310 cm (orange colour).

Nessim and Tadros (1986), Fig. 7, explained the distribution of water transparency in June 1985 in Western Harbour (Inner Harbour region and Outer Harbour region), while the other regions of the study area were extrapolated. Light penetration measurements in the Harbour water showed low values in Outer Harbour 100 cm (deep beige colour) and 110 cm in Inner Harbour (very pale green colour). Polluted areas near the outlets at El-Umum area and El-Noubaria Canal showed turbid water where water transparency did not exceed 50 cm (green colour). Considerable to the plankton bloom contributes to the relative low transparency of the Harbour water.

In general, the region in front of Alkali-Chemicals Company outfall and El-Umum Drain showed low transparency at all times. Maximum transparency was found at offshore area of El-Dekhela Harbour region. Generally, transparency increased in a seaward direction but not with time.

4.3. Salinity distribution

Surface distribution of salinity recorded in August, 1983 after Aboul-Dahab (1985) was shown in Fig. (8). In El-Mex 1 region, salinity increases readily from

the coast to the seaward direction. Maximum salinity 38.21‰ (red colour) was found in El-Dekhela Harbour region, while minimum surface salinity 16.15‰ (orange colour) was found in front of El-Umum Drain. The inshore surface salinity was always minimal next to the larger magnitude of the drain outflow water from the two sources El-Umum Drain and the Alkali-Chemicals Company outfall. The effects of Alkali-Chemicals Company are relatively restricted to a small area in vicinity of the main sources.

In Fig. (9), surface distribution of salinity recorded in April 1990 after El-Sarraf (1991) showed that the low water salinity 10‰ (orange colour) found in El-Mex 2 region and intermediate water salinity 32‰ (red colour) found in El-Dekhela region and the salinity increased to be 39‰ towards the open sea (pink colour) while the other regions in the study area were extrapolated.

In Fig. (10), surface distribution of water salinity recorded in August 1994 after Fahmy ***et al***. (1997) was studied; the distribution pattern of salinity of El-Mex 1 region and El-Dekhela Harbour region have the same pattern and high salinity 26‰ (pink colour). It was found also that El-Mex 1 region was characterized by a wide surface salinity variations, fluctuating between low and high values <12‰ in the vicinity of El-Umum Drain (yellow colour) and was gradually increased to the seaward to reach a maximum value of 27.5‰ (red colour) in the northern and northwestern side of El-Mex Bay. The surface salinity variations in El-Dekhela Harbour were limited (ranging from 25 to 26‰, pink colour).

The vertical salinity distribution showed that the effect of the discharged fresh water was pronounced in the whole water column in the vicinity of El-Umum Drain.

5. Visual interoperation

5.1. Total suspended matter distribution

The three dates of images; 1983, 1985 and 1991, shown in Figs. (11, 12 and 13) are results to the application of the algorithm of Ritchie ***et al***. (1987) to get the distribution of total suspended matter on the study area through these periods.

According to this algorithm, three bands 4, 6 and 7 are used to calculate TSM as shown in the following:

$$TSM = -34.84 + 2.44 * Band\ 4 + 6.94\ Band\ 6 - 3.55 * Band\ 7 \quad (mg\ \ell^{-1})$$

The result of this algorithm gave a weak correlation between the images and the *in-situ* measurements, so some development was to become:

$$TSM = -34.84 + 2.44 * Band\ 4 + 6.94 * Band * 6 + 3.55 * Band\ 7 \quad (mg\ \ell^{-1})$$

The coefficient of determination $r^2 = 0.99$.

In 1983, as shown in Fig. (11), high concentration of TSM in the coastal area in El-Mex 2, El-Dekhela and El-Dekhela Harbour regions up to 14.52 mg ℓ^{-1} (red colour) was recorded as well as high concentration of TSM in the Inner Harbour up to 14.52 mg ℓ^{-1} (red colour). Low concentration of TSM in Outer Harbour region and El-Mex 1 region (4.42 mg ℓ^{-1} - green colour). Intermediate concentration (7.4 mg ℓ^{-1} - yellow colour) relative to other regions was found in the front of El-Umum Drain as a bloom, very low level (1.99 mg ℓ^{-1} - blue colour) of TSM was found in the offshore area.

In 1985, as shown in Fig. (12), high concentration level was found in the coastal area in front of El-Umum Drain and in El-Dekhela region (16.23 mg ℓ^{-1} - red colour). Yellow colour and pale green colour (12.25 mg ℓ^{-1} and 10.6 mg ℓ^{-1} , respectively) were found in the region of El-Dekhela Harbour which is relatively high in comparison with 1983 imagery and that which occurred after new Harbour construction.

After few years in 1991, as shown in Fig. (13), El-Dekhela Harbour region had TSM concentrations of 17.29 mg ℓ^{-1} (red colour) more than that in the other parts of study area, and high concentrations also are observed in front of El-Umum Drain. Inner Harbour and Outer Harbour regions have a low-level (12.81 mg ℓ^{-1} - yellow colour) compared with El-Dekhela Harbour region. The construction of El-Dekhela new Harbour made the study area more closed and prevents the renew of water, so the total suspended matter has been increased.

The distributions of TSM concentrations are following the same distribution as shown by Aboul-Dahab (1985) and Fahmy ***et al.***(1997) and compatible with data derived from satellite imagery.

5.2. Transparency distribution

The three dates of images 1983, 1985 and 1991 are involved in the application of the algorithm of Shimoda ***et al.*** (1986) to get the distribution of transparency on the study area through these periods. This algorithm works using the four bands of MSS as follows:

$$Transparency = 107.591 + 0.24165 * Band\ 4 - 0.63496 * Band\ 5 - 1.4189 * Band\ 6 + 1.3171 * Band\ 7 \quad (cm)$$

The coefficient of determination $r^2 = 0.88$

In 1983, as shown in Fig. (14), low transparency was found near to the coast of El-Dekhela Harbour, El-Dekhela, Inner Harbour and El-Mex 2 regions 190 cm (green colour). The higher transparency was found in the northern part of the study area 420 cm (red colour).

In 1985, as shown in Fig. (15), low transparency was found in the coastal area in El-Dekhela region 171 cm (pale green colour), and increased gradually towards offshore area 205 cm (yellow colour). Western Harbour had a high transparency 293 cm (orange colour) relative to El-Dekhela Harbour region, generally transparency was lower than that estimated in 1983.

In 1991, as shown in Fig. (16), transparency was lower in the study area except in the virtual bloom of El-Umum Drain. Low transparency was found in the coastal area in El-Dekhela Harbour region 45 cm (green colour), and increasing gradually in the direction of the open sea 197 cm (orange colour). Inner Harbour had a transparency 113 cm (yellow colour). Generally, transparency was lower than the level estimated in 1983 and 1985. Transparency decreased from date to date due to the construction activity and the operation of El-Dekhela Harbour.

The transparency distribution that was performed by Aboul-Dahab (1985), Nessim and Tadros (1986) and El-Sarraf (1991) and compatible to the data derived from satellite imagery.

5.3. Salinity distribution

Khorram and Cheshire (1985) generated a three simulated model using Landsat MSS digital data to map salinity distribution. This algorithm is using the visible region bands of Landsat MSS:

$$Salinity = 83.524 - 120.858 * \{Band\ 6 / (Band\ 4 + Band\ 5)\} \quad (‰)$$

The application of this algorithm to the study area introduce correlation coefficient of determination $r^2 = 0.78$. So, we used this algorithm to map salinity distribution at the study area.

Salinity was estimated for the same three dates 1983, 1985 and 1991 and the results are shown in Figs. (17, 18 and 19).

In 1983, as shown in Fig. (17), low salinity value was found in coastal area of El-Mex 1, El-Dekhela and El-Dekhela Harbour regions 23.36‰ (green colour). Also, salinity values increased gradually towards the open sea 34.4‰ (yellow colour). El-Mex 2 region has a low salinity, spatial the front of El-Umum Drain at bloom 22.8‰ (pale green colour). Inner Harbour and Outer Harbour regions have the very low salinity 21.9‰ (blue colour) because the effect of several factors, such as the water exchange between open sea and the Western Harbour, the disposed sewage, domestic, industrial and freshwaters in addition to rainfall and other physical and climate conditions (Aboul-Dahab, 1985).

In 1985, as shown in Fig. (18), salinity was very low in El-Dekhela Harbour and El-Dekhela regions (blue colour) increasing very slowly to reach 19.44‰ (green colour) in the direction of open sea. El-Mex 2 region has very low salinity (blue colour) specially in the front of El-Umum Drain. Also, the Inner Harbour region has low salinity. El-Mex 1 and Outer Harbour regions have high salinity values 25.52‰ (yellow colour) compared with the other regions of the study area.

In 1991, as shown in Fig. (19), low salinity was found in the coastal area in all study area (pale green colour) then it increased gradually in the direction of the open sea 25.7‰ (yellow colour). Also, Inner Harbour and Outer Harbour regions have low salinity compared with other regions (deep beige colour). Low salinity was common in all the study area, and the virtual flux of drainage discharge water are shown as a bloom in the front of El-Umum Drain.

The construction of El-Dekhela Harbour made the study area environmentally unstable area. The record of salinity that was done by El- Sarraf (1991) and Fahmy ***et al.***(1997) are compatible to the data derived from satellite imagery.

6. Statistical analysis

6.1. Total suspended matter

Figure (20a, b and c) represents histograms of data - that released from the applied algorithm - at 1983, 1985 and 1991. Histograms shown increasing in the mean value of TSM in the study area. In 1983, 74.39 mg ℓ^{-1}. In 1991 this value is 123.64 mg ℓ^{-1}.

On the other hand, first order regression model between Aboul-Dahab (1985) and resulted image 1985 are represented graphically by Fig. (21).

Correlation coefficient (r = 0.992) proofs that positive correlation between algorithm data and digital image processing (DIM). Figure (21) shows the regression line function between the measured TSM and calculated TSM concentration by used algorithm.

6.2. Water transparency

Figure (22 a, b and c) represents histogram of the data -that released from the applied algorithm- at 1983, 1985 and 1991. Histograms shown in decreasing value of water transparency in the study area with time caused by increasing TSM resulted by the construction of El-Dekhela Harbour which closed the west area of study area in 1983, the mean value of water transparency is estimated 111.32 cm, in 1991 this value is 75.9 cm.

Figure (23) shows the regression line function between the measured transparency and calculated water transparency by used applied algorithm. On the other hand, first order regression model between Aboul-Dahab (1985) and resulted image (1983) are represented graphically by Fig. (23).

Correlation coefficient (r = 0.89) proofs that positive correlation between algorithmic data and DIM.

6.3. Water salinity

Figure (24 a, b and c) represents histograms of imagery data - that released the applied algotithm at 1983, 1985 and 1991. Histogram shown unfortified increasing in the mean value of water salinity in the study area in 1983, the mean value of water salinity was estimated 37.71‰, the same parameter was estimated 39.6‰ through after Harbour construction. On the other hand, first

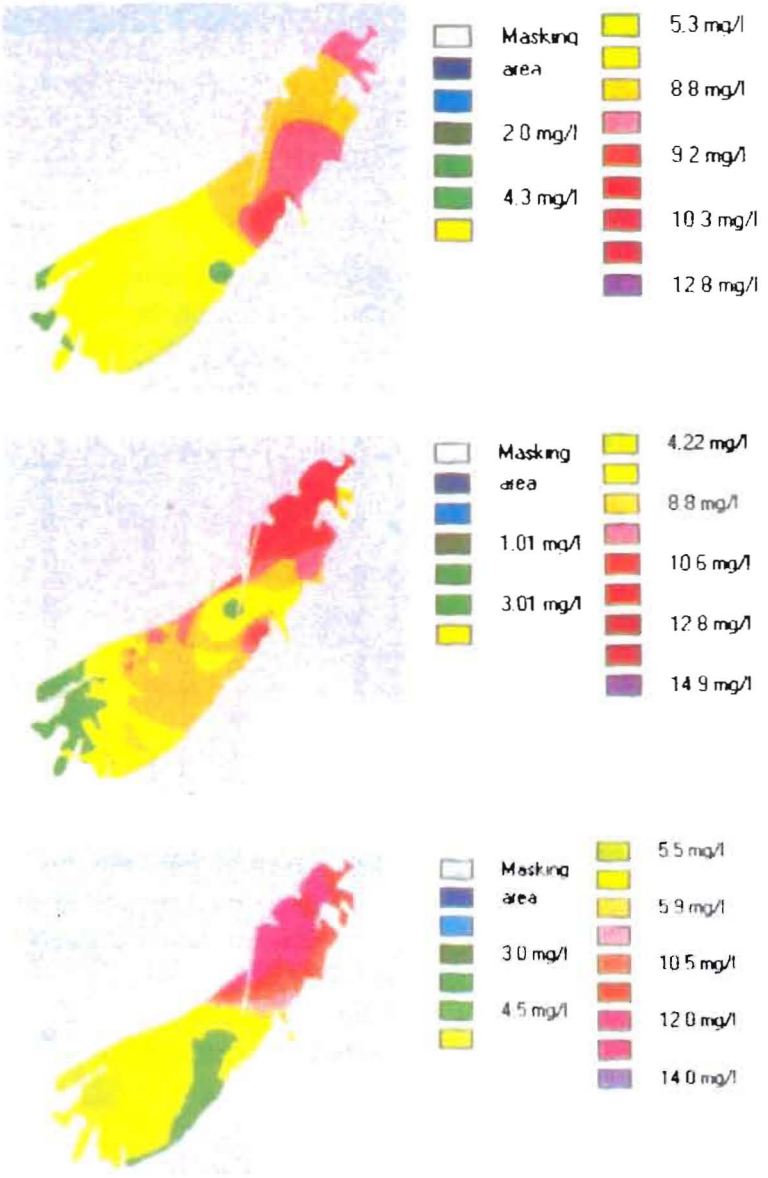

Fig. (2,3,4): TSM, August (1994) (After Fahmy, *et al.*, 1997).

Fig. 5 Water Transparency , August 1983 , *(After Aboul Dahab, 1985)*

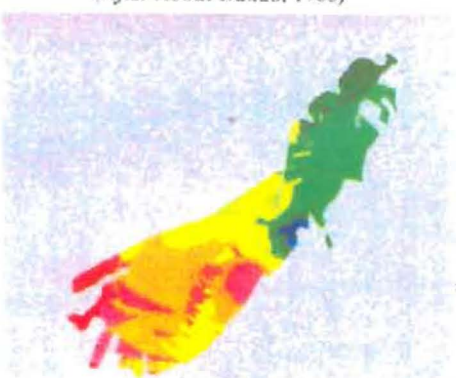

Fig. 6 Water Transparency, August 1984, *(After Aboul-Dahab, 1985)*

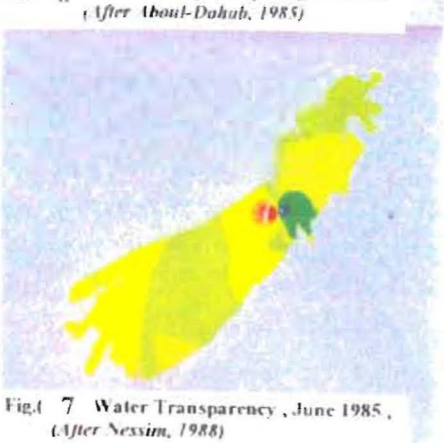

Fig. 7 Water Transparency , June 1985 , *(After Nessim, 1988)*

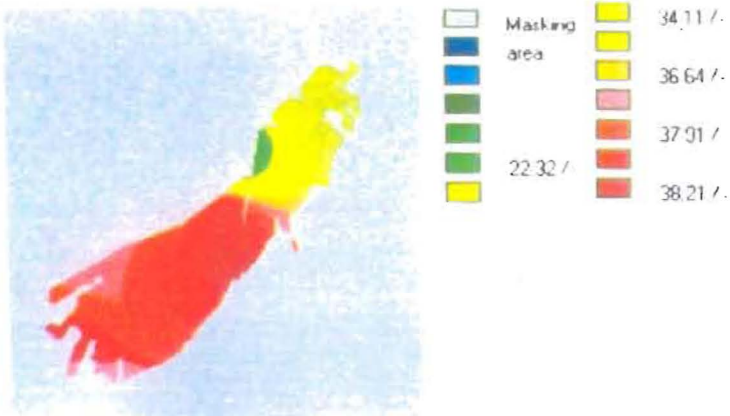

Fig. 8) Water Salinity, August 1983.
(After Aboul-Dahab 1985)

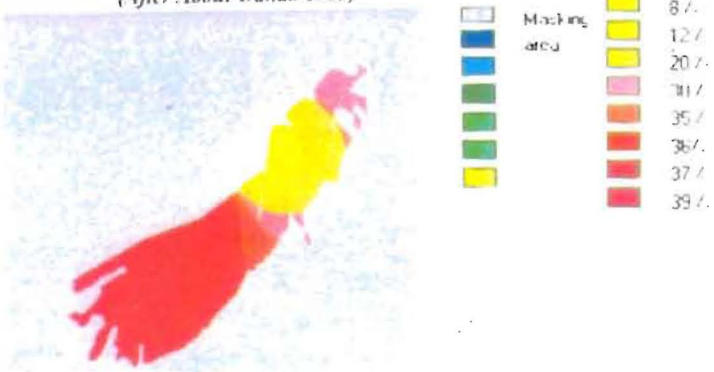

Fig 9) Water Salinity, April 1990.
(After El-Sarraf 1991)

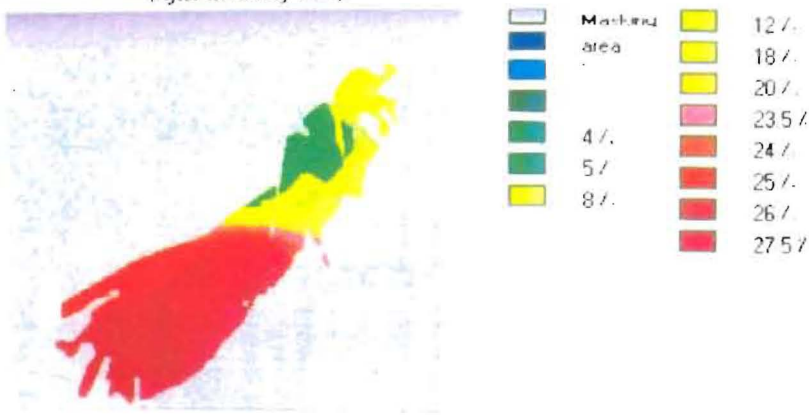

Fig 10 Water Salinity, August 1994.
(After Fahmy 1997)

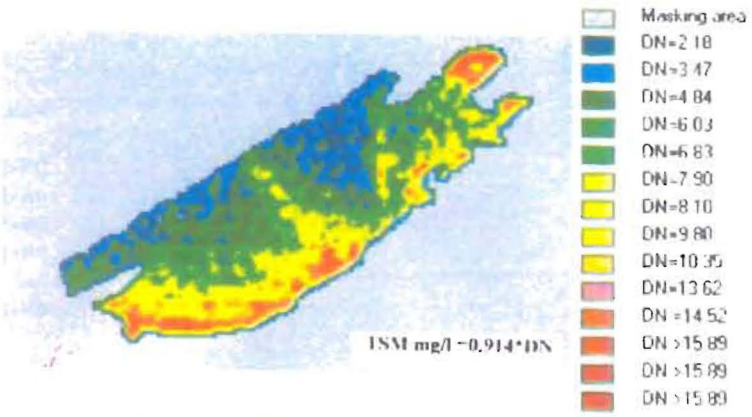

Fig. 11 Total Suspended Matter at July 1983.

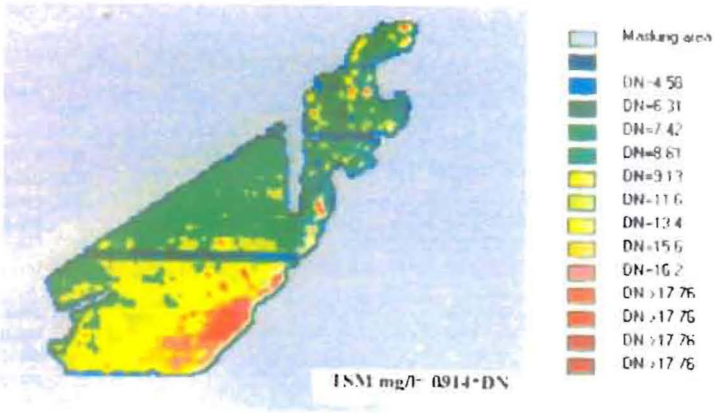

Fig. 12 Total Suspended Matter at June 1985.

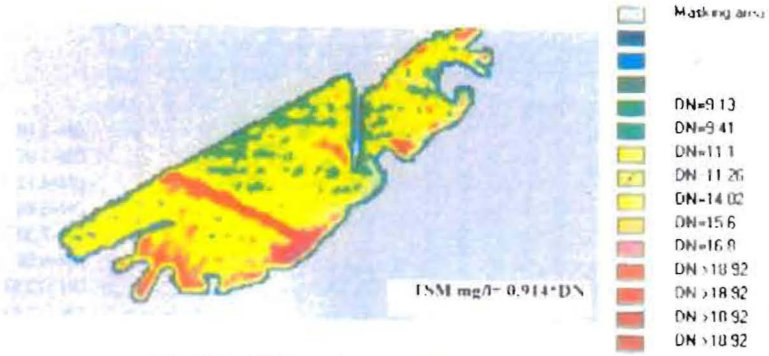

Fig. 13 Total Suspended Matter at February 1991.

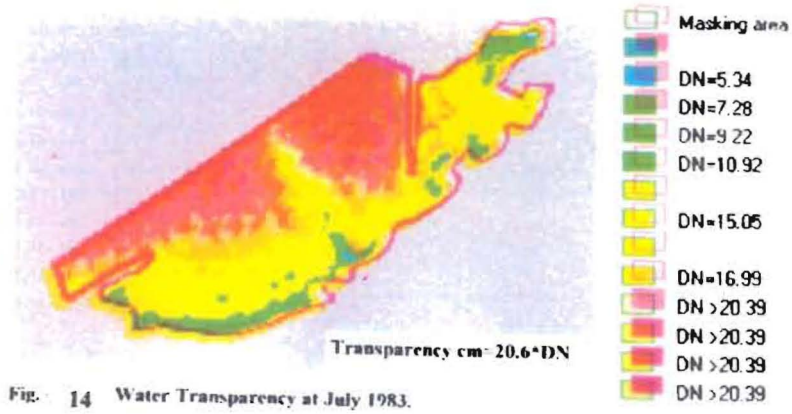

Fig. 14 Water Transparency at July 1983.

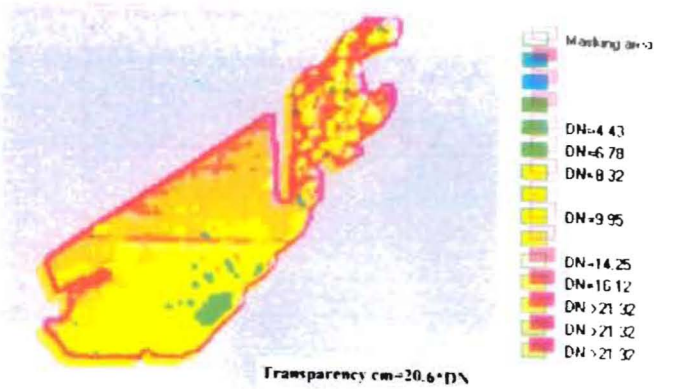

Fig. 15 Water Transparency at June 1985.

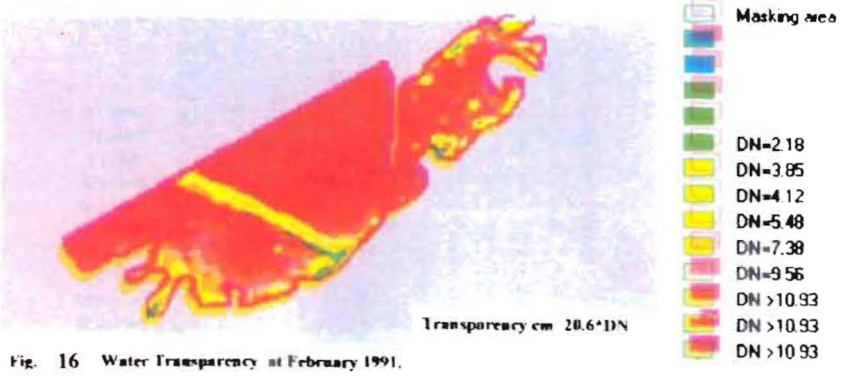

Fig. 16 Water Transparency at February 1991.

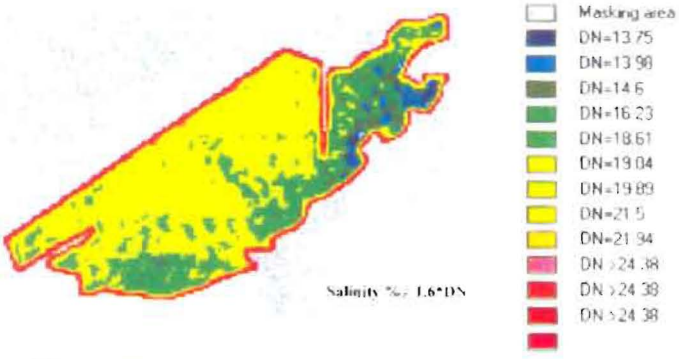

Fig. (17 ater Salinity at July 1983.

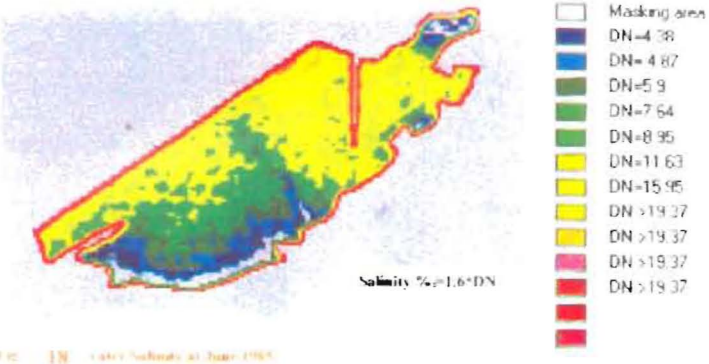

Fig. 18 Water Salinity at June 1985

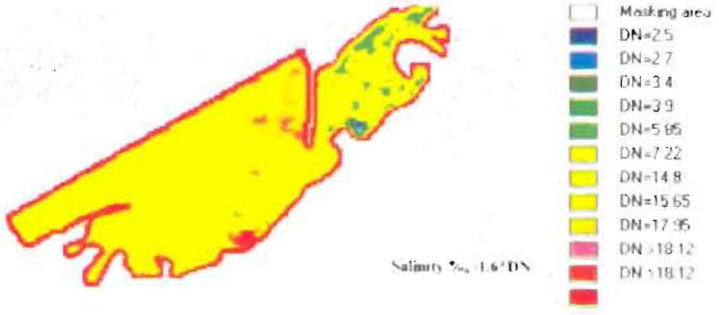

Fig. 19 Water Salinity at February 1991

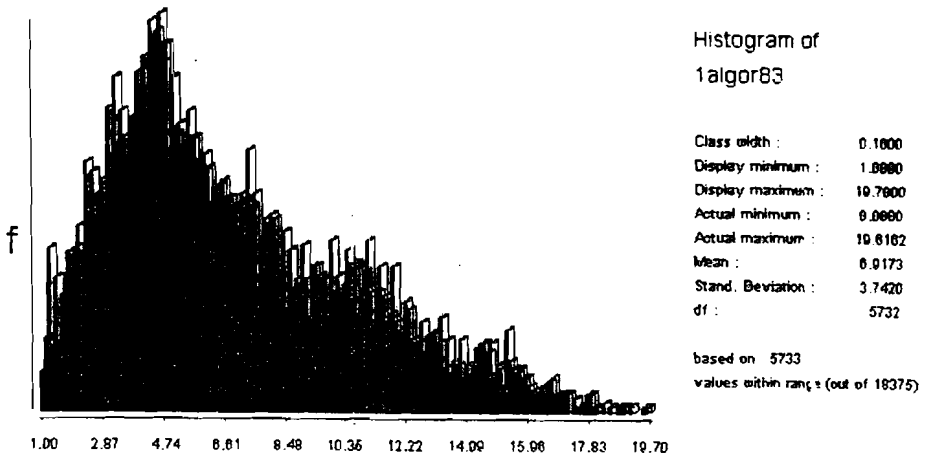

Fig. (20a): Histogram of Total Suspended Matter distribution (mg/l) in 1983.

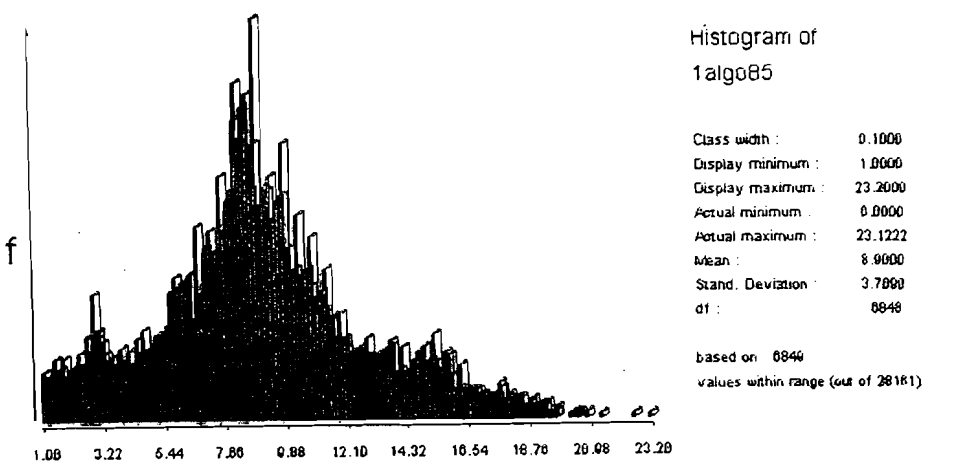

Fig. (20b): Histogram of total Suspended Matter distribution (mg/l) in 1985.

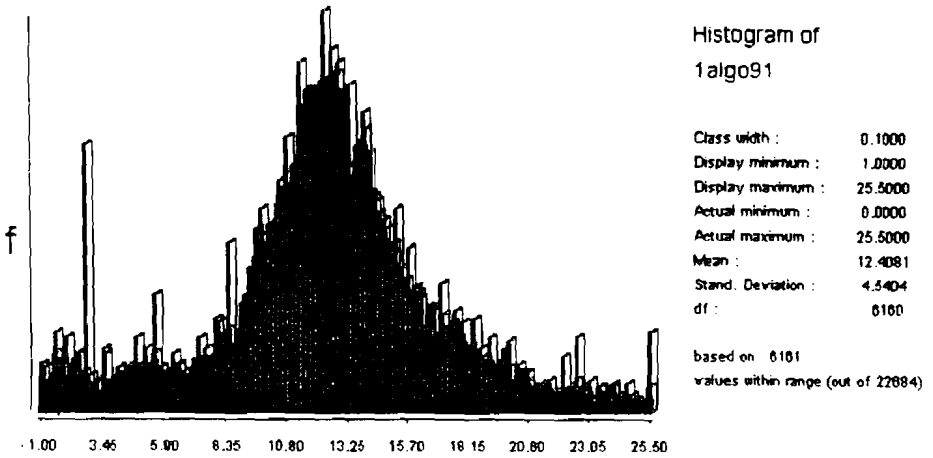

Fig. (20c): Histogram of total Suspended Matter distribution (mg/l) in 1991.

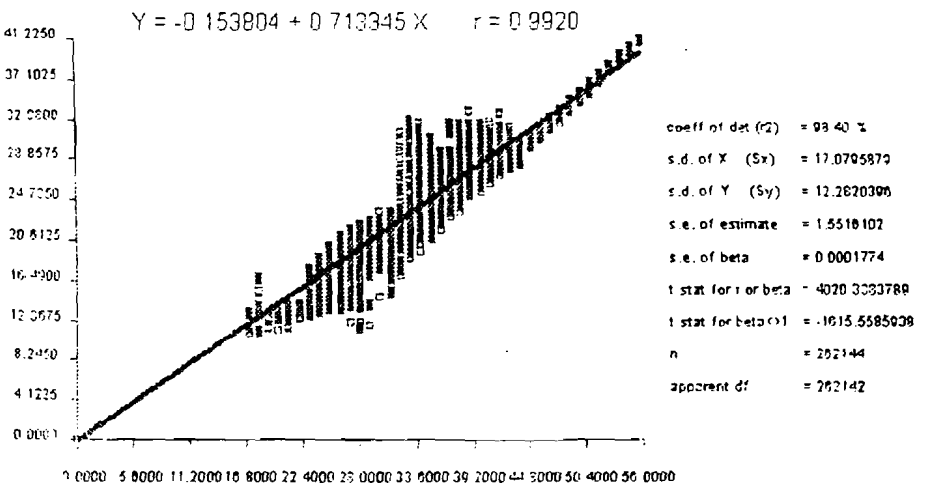

Fig. (21): Scatter plot between Total Suspended Matter of ground measurement {(Aboul-Dhab (1985)}, and Total Suspended Matter resulted from applied algorithm (1985)

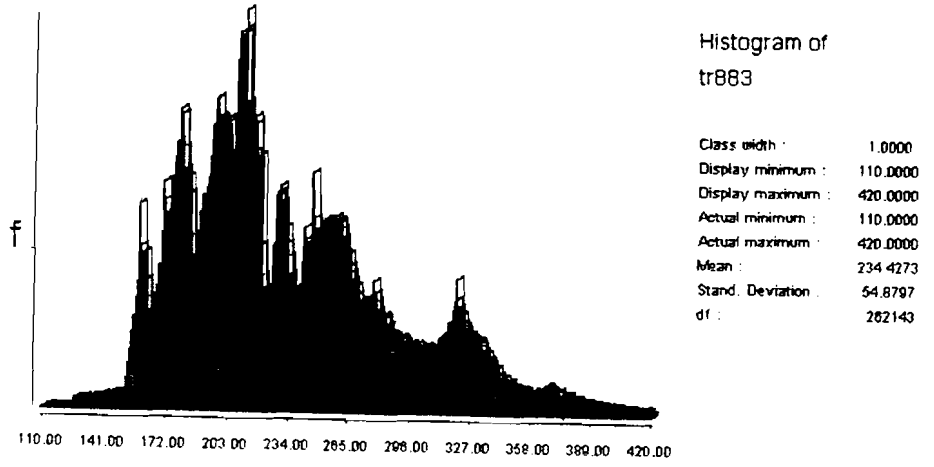

Fig. (22a): Histogram of Water Transparency distribution (cm) in 1983.

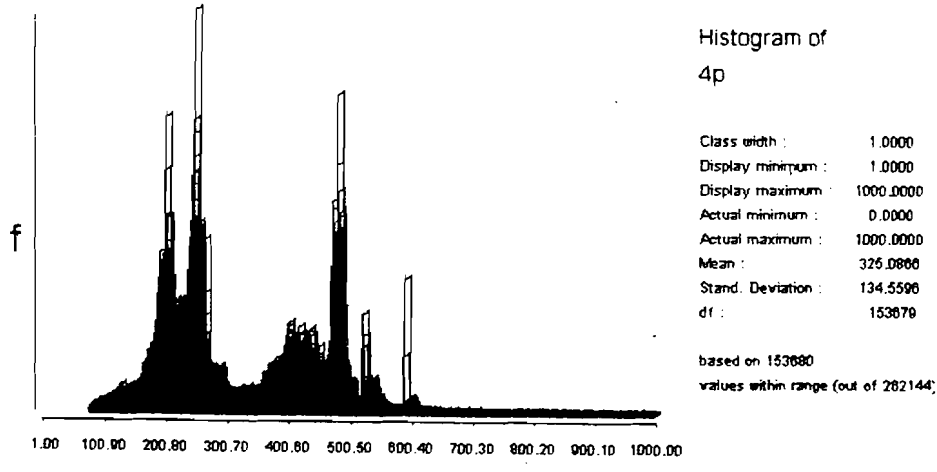

Fig. (22b): Histogram of Water Transparency distribution (cm) in 1985.

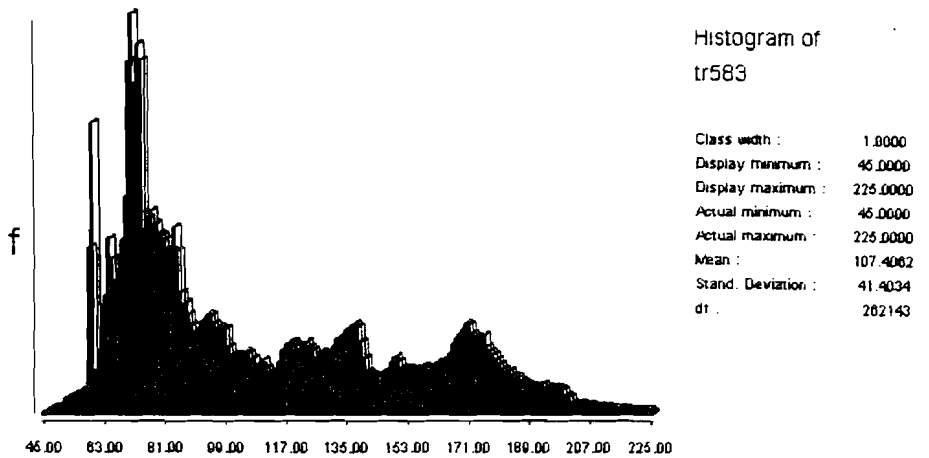

Fig. (22c): Histogram of Water Transparency distribution (cm) in 1991.

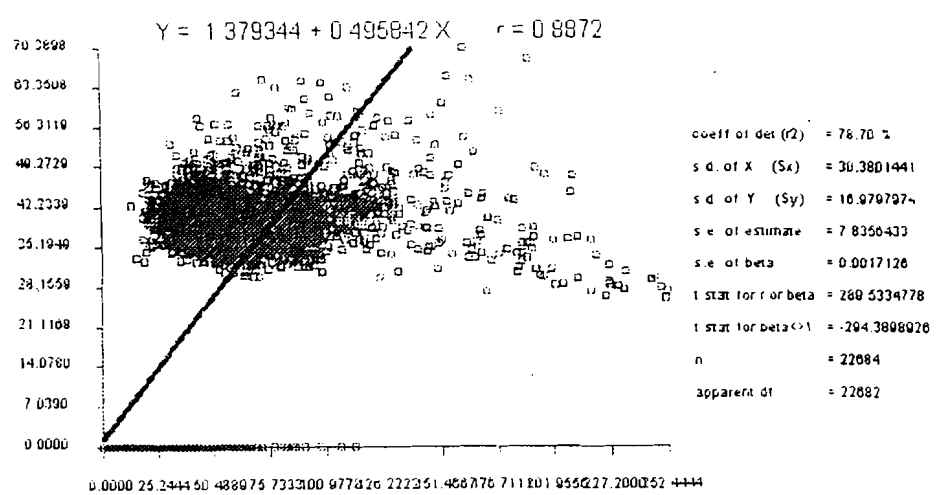

Fig. (21): Scatter plot between Water Transparency of ground measurement {(Aboul-Dhab (1985)}, and Water Transparency resulted from applied algorithm (1985)

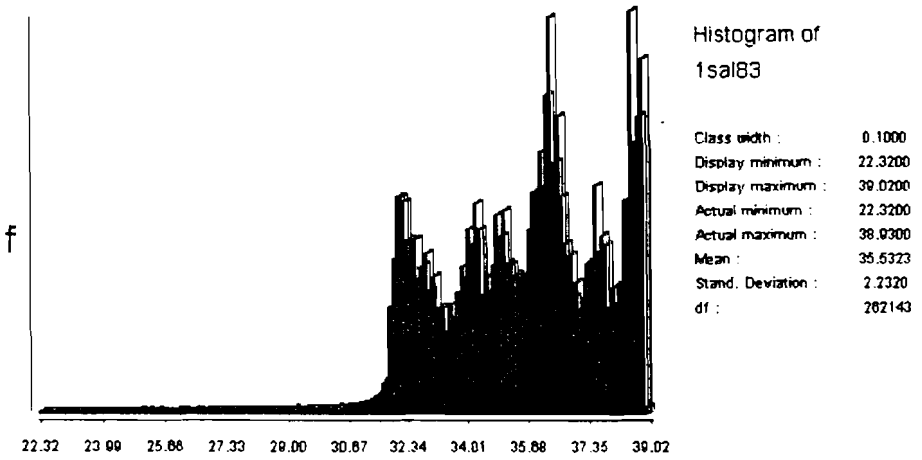

Fig. (24a): Histogram of Water Salinity distribution (‰) in 1983.

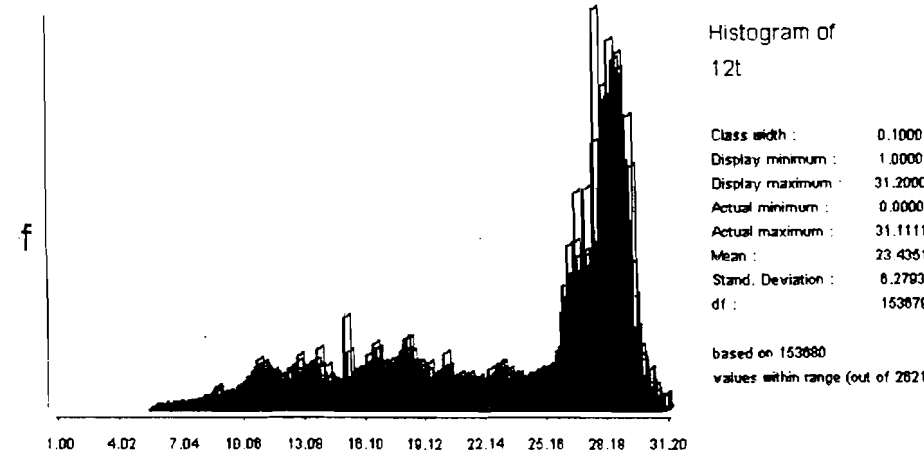

Fig. (24b): Histogram of Water Salinity distribution (‰) in 1985.

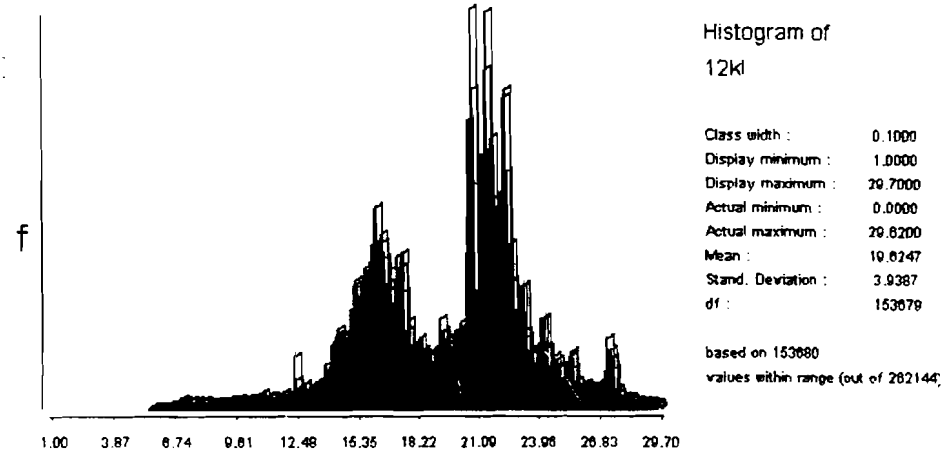

Fig. (24c): Histogram of Water Salinity distribution (‰) in 1991.

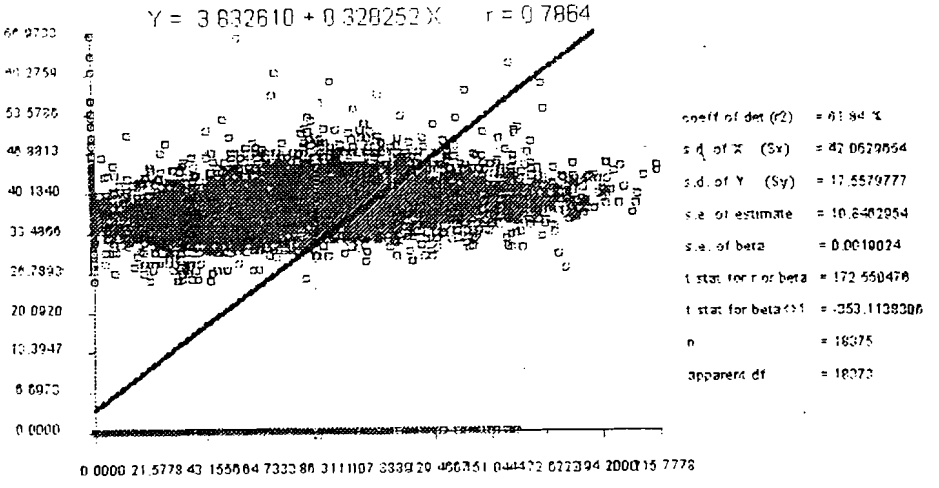

Fig. (25): Scatter plot between Water Salinity of ground measurement {Fahmy (1997)}, and Water Salinity resulted from applied algorithm (1991).

order regression model between Fahmy ***et al.*** (1997) resulted image 1991 are represented graphically by Fig. (25).

Correlation coefficient (r = 0.78) proofs that positive correlation between algorithmic data and DIM.

The statistical analysis proofs that there is a significant positive correlation between imagery data - that derived from satellite imagery - using specific algorithm and digital interpolation model based on the *in situ* measurements. This correlation leads to that both processed satellite imagery and digital interpolation model lead to the same results.

7. Conclusion

Finally, from this study we can conclude that the validity of remote sensing technique when compared with the ground measurements were 78%, 88% and 99% for salinity, transparency and TSM, respectively. The applied algorithm is a useful tool to determine the water quality parameters selected in this study instead of the traditionally used methods and the rate of change has increased after the establishment of El-Dekhela New Harbour.

REFERENCES

Abd-Alla, R.R.; Zaghloul, F.A.; Hassan, Y.A. and Moustafa, H.M.; 1995. Some water quality characteristics of El-Dekhela Harbour, Alexandria, Egypt. Bull. Nat. Inst. Oceanogr. & Fish., ARE, 21 (1): 85-102.

Aboul-Dahab, O.M.T.; El-Rayis, O.A. and Halim, Y.C.; 1984. Environmental conditions in Mex Bay, west of Alexandria. 1- Physical speciation of four trace metals in the Bay. VII^{es} Journees Etude. Pollution, Lucerne, C.I.E.S.M., pp. 347-355.

Aboul-Dahab, O.M.T., 1985. Chemical cycle of inorganic pollutants in the ecosystem west of Alexandria between Anfoushy and Agamy. Ph.D. Thesis, Faculty of Science, Alexandria University.

Alexandria Port Authority, APA, 1996. Ministry of Maritime Transport. Special report for description of the harbour. (In Arabic).

APHA (1982). Standard Methods for the Examination of Water and Waste Water. 15th Ed., American and Public Health Assoc., Washington, 1009 pp.

Austin, R.W., 1974. The remote sensing of spectral radiance from the ocean surface. In optical aspects of oceanography, T. Platt: 317-344.

Central Authority for Mobilization and Statistics, CAMS, 1996. General census for 1994. Population Characteristics, Alexandria Governorate. No. 913/97/MAT. (In Arabic).

Cracknell, A.P.; Karniel, A. and Huang, W.Q.; 1988. Water quality off the west coast of Ireland studied from satellite images. International Journal of Remote Sensing, 9 (3): 439-446.

El-Sarraf, W.M., 1991. Water quality of the Mediterranean coastal marine environment in front of Alexandria, Egypt. Bull. Nat. Inst. Oceanogr. & Fish., ARE, 17 (1): 25-30.

Emara, H.I.; Iskander, M.F. and Assad, F.N.; 1984. Chemistry of sea water west of Alexandria. Bull. Nat. Inst. Oceanogr. & Fish., ARE, 10: 35-49.

Fahmy, M.A.; Tayel, F.T. and Shriadah, M.M.; 1997. Spatial and seasonal variations of dissolved trace metals in two contaminated basins of the coastal Mediterranean Sea, Alexandria, Egypt. Bull. Fac. Sci., Alex. Univ., 37 (2): 18-29.

Halim, Y., 1983. Mid-term Report: Aquatic environmental pollution project EGY 173/058. Alexandria University.

Khorram, S. and Cheshire, H.M., 1985. The use of Landsat MSS digital data in water quality mapping of the Neuse River Estuary, North Carolina. Photogramm. Eng. Rem. Sens., 4 (2): 83-193.

Kindratyev, K.Y.; Pozdnyakov, D.V. and Petterson, L.H.; 1998. Water quality remote sensing in the visible spectrum. Int. J. Rem. Sens., 19: 957-979.

Nessim, R. B., 1994. Environmental characteristics of Mex Bay 1st Proc. Arab Conf. on Marine Environment Protection. Alexandria, 221-243.

Nessim,R.B. and Tadros, A. B., 1986. Distribution of nutrient salts in the water and pore water of the Western Harbour of Alexandria, Egypt. Bulletin of Institute of Oceanography & Fisheries, ARE, 12: 165-174.

Okbah, M.A., 1999. Speculation of some trace metals (Fe, Cu and Cd) in El-Mex Bay water, Alexandria, Egypt. INQUA Newsletter No. 21, Spain, pp. 124-136.

Richardo, J., 1993. Using MSS data to estimate total suspended matter in Vira Groth Harbour. Eng. Rem. Sens., 69 (7): 74-101.

Ritchie, J.C.; Cooper, C.M. and Yongqing, J.; 1987. Using Landsat Multispectral Scanner data to estimate suspended sediments in Moon Lake, Mississippi. Rem. Sens. Environ., 23: 65-81.

Robinson, I.S., 1985. Satellite Oceanography. An Introduction for Oceanographers and Remote Sensing Scientists, Ellis – Horwood, Limited.

Said, M.A.; El-Deek, M.S.; Mahmoud, Th.H. and Shriadah, M.M.A.; 1991. Physico-chemical characteristics of different water types of El-Mex Bay, Alexandria, Egypt. Bull. Nat. Inst. Oceanogr. & Fish., ARE, 17 (1): 103-116.

Schnider, K. and Mauser, W., 1996. Processing and accuracy of Landsat Thematic Mapper data for lake surface temperature measurements. Int. J. Rem. Sens., 17 (11): 2027-2041.

Shimoda, H.; Etaya, M.; Sacata, T.; Goda, L. and Stelczer, K.; 1986. Water quality monitoring of Lake Balton using Landsat MSS data. Symposium on Remote Sensing for Resources Development and Environmental Management / Enschede/: 545-560.

Tayel, F.T.; Fahmy, M.A. and Shriadah, M.A.; 1996. Studies on physico-chemical characteristics of the Mex Bay and new Dekhela Harbour of Alexandria. Bull. Nat. Inst. Oceanogr. & Fish., ARE, 22: 1-18.